A Study of Surface Film Formation on $LiNi_{0.8}Co_{0.15}Al_{0.05}O_2$ Cathodes Using Attenuated Total Reflection Infrared Spectroscopy

S.-W. Song [a,*], G. V. Zhuang [b,*,z] and P.N. Ross, Jr. [b,*]
[a] Environmental Energy Technologies Division
[b]Materials Sciences Division
Lawrence Berkeley National Laboratory
Berkeley, CA 94720, USA

Abstract

The surface films formed on commercial $LiNi_{0.8}Co_{0.15}Al_{0.05}O_2$ cathodes (ATD Gen2) charged from 3.75V to 4.2V vs. Li/Li^+ in EC:DEC - 1M $LiPF_6$ were analyzed using ex-situ Fourier transform infrared spectroscopy (FTIR) with the attenuated total reflection (ATR) technique. A surface layer of Li_2CO_3 is present on the virgin cathode, probably from reaction of the active material with air during the cathode preparation procedure. The Li_2CO_3 layer disappeared even after soaking in the electrolyte, indicating that the layer dissolved into the electrolyte possibly even before potential cycling of the electrode. IR features only from the binder (PVdF) and a trace of polyamide from the Al current collector were observed on the surfaces of cathodes charged to below 4.2 V, i.e. no surface species from electrolyte oxidation. Some new IR features were, however, found on the cathode charged to 4.2 V and higher. An electrolyte oxidation product was observed that appeared to contain dicarbonyl anhydride and (poly)ester functionalities. The reaction appears to be an indirect electrochemical oxidation with overcharging (removal of > 0.6 Li ions) destabilizing oxygen in the oxide lattice resulting in oxygen transfer to the solvent molecules.

[*]Electrochemical Society Active Member
[z]Author to whom all correspondence should be addressed.
Phone: +1-510-486-4793
Fax: +1-510-486-5530
Email:GVZhuang@lbl.gov

Introduction

Lithium-ion cells generally exhibit a relatively large (ca. 15-20 %) irreversible loss of capacity during the initial few cycles. Research in the last decade has established that most of this irreversible capacity loss is due to the formation of the so-called solid-electrolyte interface layer (SEI) on graphite and other carbon-based negative electrodes[1-11]. These irreversible reactions are comprised of electrochemical reductions of the electrolyte below the potential ca. 1.5V vs. Li/Li^+, but the specific reactions occurring and specific composition of the SEI layer in commercial cells has been difficult to establish, and complicated by adventitious impurities introduced during processing and assembly[11]. There have also been reports of irreversible capacity loss on the first few cycles with $LiCoO_2$ and $LiMn_2O_4$ cathodes[12-17]. There have been several reports that an SEI layer also forms on cathodes such as $LiCoO_2$, $LiMn_2O_4$, and $LiNi_{1-x}Co_xO_2$ from electrolyte oxidation[18-25], although the nature of the reactions is unclear. More recently, Abraham and co-workers[26] proposed formation of an oxygen deficient surface layer on a $LiNi_{1-x}Co_xO_2$ cathode as a result of oxygen transfer reactions with the electrolyte. A variety of spectroscopic methods have been applied *ex-situ* to analyze surface films formed on Ni, Co and Mn-based cathodes harvested from cells, including NMR[22], XPS[23] (x-ray photoelectron spectroscopy) and XAS[21,24,26] (x-ray absorption spectroscopy), but the results were only suggestive not conclusive.

Recently, *ab-initio* density functional theory (DFT)[27] was used to examine the energetics of electrochemical oxidation of common battery solvents, including EC and DEC and DMC. The thermodynamic potentials calculated for the initial one-electron ionization to form a radical cation are 5.58 V (vs. Li/Li^+) for EC and 5.46 V for DEC (or

DMC, there is very little difference). The experimental oxidation potential values reported in the literature vary significantly. It appears that the solvent oxidation potential can be influenced by composition of the cathode materials as well as the salt used in the electrolyte. Impurities, particularly water, may also play an important role. Another source of variability in the experimental measurement of the oxidation potential is the arbitrary criteria used for determining the onset of anodic current. In general, with inert electrodes like glassy carbon or Pt, the experimental oxidation potentials for the common carbonate electrolytes are above 5 V (see Table V in ref. 27), but there are exceptional reports even in recent literature.

Of particular relevance here are the recent conflicting reports on the oxidation potential for EC-based electrolytes by Aurbach and co-workers[28] and Joho and Novak[29]. While Aurbach and co-workers studied many more solvent-salt combinations than Joho and Novak, they did have one electrolyte in common, 1:1 EC:DMC – 1 M $LiPF_6$, yet reported dramatically different oxidation potentials using similar detection methods (*in-situ* IR spectroscopy). Aurbach and co-workers reported an oxidation potential below 4 V for this electrolyte using Pt, Au and Al as electrodes, while Joho and Novak reported an oxidation potential above 5 V. Joho and Novak noted a strong effect of water on the oxidation potential (lowering), but it is not clear that adventitious water is the explanation for the discrepancy. Kanamura and co-workers[14-16] have also studied electrolyte oxidation reactions with in-situ IR spectroscopy using PC with a variety of salts and different electrode materials. When using Pt or Au electrodes[14], they observed the onset of PC oxidation at potentials above 5 V, but with $LiCoO_2$ electrodes[16] they detected multiple products attributed to a PC ring opening reaction that was initiated at

4.2 V in all three salts, $LiClO_4$, $LiBF_4$, and $LiPF_6$. Kanamura and co-workers have termed the reaction of PC with $LiCoO_2$ in the 4.2 – 4.8 V region as a "catalytic" reaction without defining this term more completely. It would appear that the thermodynamic potential for oxidation of carbonates like EC, PC and DEC/DMC by (outer-sphere) one-electron ionization to form the radical cation is indeed in the region of 5.5 – 6 V as calculated by DFT, but that other oxidation reactions are also possible, and these may occur at lower potential due to specific interactions (the "catalytic" effect) with the electrode surface, e.g. the lattice oxygen.

Recently, we reported high quality IR spectra of the passive film on graphite anodes obtained *ex-situ* using the attenuated total reflection (ATR) technique[30]. The graphite anodes were harvested from an 18650-type lithium cell with a $LiNi_{0.8}Co_{0.15}Al_{0.05}O_2$ cathode, the same cathode material studied here, following calendar aging[31] (60% state of charge) at 55 ^{o}C as part of the ATD program managed by DOE.[32] There were no IR features of surface species (solvent oxidation products) observable on the cathode. These cathodes were, however, rinsed in DMC before analysis, and soluble oxidation products (as reported by Kanamura et al [16]) would have been washed off. In the present work, we report a more detailed study using *ex-situ* ATR-IR spectroscopy of the $LiNi_{0.8}Co_{0.15}Al_{0.05}O_2$ cathode material following electrochemical characterization in half cells *vs*. a Li counter electrode and varying washing time with DMC. It is shown that indeed there is a surface reaction between EC:DEC and $LiNi_{0.8}Co_{0.15}Al_{0.05}O_2$, but only at 4.2 V or higher, and no reaction was observed at the potential region corresponding to the 60 % state of charge used in the

calender aging of the 18650 cells. We also show that the reaction product at 4.2 V is soluble in DMC and is removed by rinsing.

Experimental

The $LiNi_{0.8}Co_{0.15}Al_{0.05}O_2$ powder cathodes (denoted henceforth as the Gen2 cathode) laminated on the 30 μm thick aluminum current collector were provided by Quallion Corp. (Sylmar, CA) and were composed of 84wt% active $LiNi_{0.8}Co_{0.15}Al_{0.05}O_2$ powders (Fuji CA 1505), 4wt% amorphous carbon (Chevron), 4wt% graphite (SFG16, Timcal) and 8wt% PVdF (polyvinylidene-difluoride) binder (Kureha).[26] The cathode laminates as received were dried at 80°C overnight in a vacuum oven before storing in the helium-filled glove box (water and oxygen content is less than 10 ppm). Electrochemical cells for the cathodes with 1 cm^2 area were assembled using Swagelok® fittings with a Li reference electrode and a Li counter electrode, and Celgard 2300 separator in 1M $LiPF_6$/EC:DEC (1:1) electrolyte (LP 40 Selectipur™ from EM Sciences) in the glove box. Identical cells were separately charged at a low rate of C/25 at room temperature using a commercial battery cycler (Arbin, College Station, TX). In each case, the cell was charged (cathode was delithiated) to 3.75 V, discharged (lithiated) to 3.0 V, then charged to final cut-off potentials between 3.75 and 4.2V vs. Li/Li^+. The cells were then held at those final potentials for two hours prior to disassembly in the glove box, and the cathodes were removed from the glove box for IR analysis. First unwashed cathodes were measured by FTIR, returned to the glove box, and then washed with DMC followed by solvent evaporation in the glove box at room temperature. IR spectra were obtained with varying washing time with DMC. For comparison, we also prepared control samples of an as-received Gen2 cathode and gold

(Au) foil soaked in the same electrolyte for 24 hrs. without applying any electrochemistry. DMC washing-time dependent IR spectra were also obtained. Under no circumstances were any of the samples subject to air exposure. All samples were transferred from the glove box to the helium-purged FTIR spectrometer sample chamber using a portable vacuum-sealed container.

The FTIR measurements were obtained with a Nicolet Nexus 870 Spectrometer equipped with a broadband Mercury-Cadmium-Telluride (MCT) detector. The spectra were acquired in the Attenuated Total Reflection (ATR) mode using a hemispherical Ge optic with spectral resolution of 4 cm^{-1} with a total of 512 scans co-added. All the spectra were obtained from a 2 mm diameter area on samples pressed against the Ge crystal. We emphasize that all the FTIR measurements were performed directly on the surface of interest without any preparation such as scraping the cathode powders from the aluminum current collector. The penetration depth of the (mid-)infrared light (2000 cm^{-1}) into a medium with n = 1.5 (an optical constant typical for organic compounds) is on the order of magnitude of 400 nm. The ATR-FTIR spectra were corrected for the light penetration depth as function of wavelength. A linear background correction was also performed to eliminate the sloping spectral background caused by surface roughness. None of the spectra shown were subjected to a "smoothing" algorithm.

Results

$LiNi_{0.8}Co_{0.15}Al_{0.05}O_2$ cathode as-recieved

Infrared spectrum of the Gen2 cathode as-received from Quallion is presented in Figure 1. Spectral comparison between the Gen2 cathode and just PVdF powder, used in laminating Gen2 cathode, shows that most of the features in the spectral region of 1300-

800 cm^{-1} could be readily attributed to PVdF. However, the strongest feature centered about 1400 cm^{-1} is much broader than that of the pure PVdF. Peak broadening and skew in the low wave number region are typical for a rough sample surface, but the feature broadening at 1400-1500 cm^{-1} is due to quite different origin. As shown by the reference spectrum of Li_2CO_3 in Figure 1, the strong peak at 1416 cm^{-1} and a shoulder at 1500 cm^{-1} could be assigned to the C-O asymmetric and symmetric stretching modes of Li_2CO_3. Li_2CO_3 also has a sharp peak at 875 cm^{-1} associated with the $(CO_3)^{-2}$ bending mode, which overlaps with spectral features from PVdF in the same region. To our knowledge, this Li_2CO_3 is not an intentional additive, but is a layer that forms on the active cathode material by reaction with CO_2 in the air during processing. This observation is not new, and in fact there has been a detailed study[33] of the reaction of this class of cathode material ($LiNi_{1-x-y}Co_xAl_yO_2$) with CO_2 in ambient air, and Andersson et al.[23] reported finding Li_2CO_3 in the as-received GEN1 cathode material (y=0).

The IR spectrum in Figure 1 also shows that lithium carbonate is not the only impurity introduced into the cathode material during processing. In the CH group frequency region of 2750 – 3250 cm^{-1} shown in Figure 2 (top), PVdF has two sharp peaks at 3020 cm^{-1} and 2982 cm^{-1} (from the olefinic =CH– group), but the most prominent peaks observed on Gen2 cathode are at 2922 and 2849 cm^{-1} characteristic asymmetric and symmetric stretching modes[34,35] of the methylene group (–CH_2–), e.g. in an alkyl or paraffin compound. To investigate the source of this impurity, we made an FTIR measurement on regions of the Al current collector which is not covered by cathode laminate. The presence of a polymer film is unmistakable from the spectrum marked as cathode foil in the lower panel of Fig.2. This IR spectrum indicates the film

contains an amide group (R-CO-NH_2). The features in the spectral region between 3100 – 3400 cm^{-1} are of the NH group frequency region. Specifically, peaks at 3352 cm^{-1} and 3183 cm^{-1} can be attributed to NH asymmetry and symmetry stretching modes of NH_2 group, respectively. The feature at ~1640 cm^{-1} is characteristic of C=O in the amide[34,35]. Judging from the relative peak intensities, the polymer is comprised of a significant number of (-CH_2-) units, although from IR one could not conclude the exact alkane chain length. There is a striking spectral resemblance between the spectrum from the cathode foil and the generic polymeric coating material oleamide, which is commonly used as a corrosion inhibitor[36]. The strong broad peak centered at 916 cm^{-1} is from the contribution of aluminum oxide. Based on the IR penetration depth of ca. 500nm and the fact we observe the aluminum oxide, the polyamide coating thickness is less than 500 nm (0.5μm). The ν(NH) modes of the polyamide are, however, not seen in the spectrum of the cathode laminate, while the ν(CH) modes are preserved. We surmise, therefore, that in solvent casting the cathode layer with n-methyl-pyrrolidinone (NMP), the polyamide film is stripped from the Al foil and a paraffin polymer is deposited in the active layer during drying of the NMP.

Spectra of Electrolyte Residue

In order to identify by ex-situ analysis surface species derived from electrochemically induced changes to an electrode, it is crucial to identify the spectral features associated with residual electrolyte. In this context, we first examined the residual electrolyte on a Au foil after it was dipped in the electrolyte. The IR spectra obtained on Au foil prior to DMC washing is shown in curve (a) and (b) in Fig.3. While some of the spectral features of DEC were discernable in spectrum (a), as indicated by

the presence of peaks at 1740 cm^{-1}, 1300 cm^{-1}, 1268 cm^{-1}, and 1015 cm^{-1}, the spectrum (b) from a different spot on the surface is consistent with pure liquid phase EC [37] with two additional features. First, the relatively strong peak at 840 cm^{-1} is not attributed to either EC or DEC but is unambiguously assigned to the P-F stretching from solvated $LiPF_6$[30]. Second, the relative intensity of two bands at 1804 cm^{-1} and 1769 cm^{-1}, unique to the EC carbonyl group, is different from that of pure solid or liquid phase EC. In solid EC, two strong peaks at 1791 and 1829 cm^{-1} of equal intensity, and are due to a Fermi resonance between C=O stretching and the overtone of the EC ring breathing mode at 895 cm^{-1}. A systematic comparison of spectra for solid EC and the residual EC on Au indicates that the ring breathing mode shifts to 904 cm^{-1} and the intensity of the ring breathing overtone at 1804 cm^{-1} is reduced as a result of the primary solvation of the $LiPF_6$ by the EC when the DEC evaporates, i.e. the residue is as expected for an EC:$LiPF_6$ solvate. All of these bands from the electrolyte residue disappeared after washing with DMC for only 20 seconds (Figure 3(c)). No significant organic species remain on the surface of the Au foil.

We then compared the spectra from the residue left on the Au foil with those on the as-received $LiNi_{0.8}Co_{0.15}Al_{0.05}O_2$ cathode soaked in electrolyte under identical conditions. The cathode soaked in the electrolyte has shown the similar spectral features (Fig.4 (c)) with that of Au foil prior to DMC washing, suggesting that cathode was covered by the same EC:$LiPF_6$ solvate. After washing with DMC (as shown by curve (d) in Fig. 4), peaks attributed to PVdF were observed, where two strong bands at 1171 cm^{-1} and 1071 cm^{-1} comes from ν(C-F), and the band at 1400 cm^{-1} from CH_2 bending. Of particular interest is the disappearance of spectral features from Li_2CO_3 on the cathode

after just soaking in the electrolyte, despite no electrochemistry applied. The strong peak at 1416 cm^{-1} and a shoulder at 1500 cm^{-1}, assigned to C-O asymmetric and symmetric stretching modes of Li_2CO_3, are clearly absent in Fig. 4(b). The Li_2CO_3 pre-existing in the as-received cathode must have been decomposed by contact with the electrolyte, probably by reaction with the Lewis acid PF_5 in equilibrium with $LiPF_6$ in this electrolyte.[41] The electrode surface to electrolyte volume ratio in this experiment was orders of magnitude higher than in a practical Li-ion battery, so it is not clear that the pre-existing Li_2CO_3 layer would be decomposed simply by reaction with the electrolyte in the cell upon assembly.

Electrochemical and Spectroscopic Characterization of $Li_{1-x}Ni0_{.8}Co_{0.15}Al_{0.05}O_2$, cathodes

Fig. 5(a) shows a voltage profile of the $Li_{1-x}Ni0_{.8}Co_{0.15}Al_{0.05}O_2$ cathode between 3.0 and 4.2V in the 1M $LiPF_6$/EC:DEC electrolyte during galvanostatic cycling at the low rate of C/25. The charge and discharge curves of this cathode, due to the continuous formation of $Li_{1-x}Ni_{0.8}Co_{0.15}Al_{0.05}O_2$ with an hexagonal structure in that voltage region, are consistent with previous results.[38] The irreversible processes are more clearly distinguished in the calculated differential capacity plots shown in Fig. 5(b). The initial charge curve shows a sharp large peak at 3.63V and a shoulder around 3.75V attributed to the Li^+ deintercalation. The peak at 3.63V shifted downward to 3.57V and became smaller on the following cycle, showing a greater peak separation. This suggests two lithium extraction processes, probably due to the structural change in this cathode materil. Although the partial substitution of Al and Co for Ni stabilizes the 2-D character of $LiNiO_2$ structure and improves the electrochemical performance,[39, 40] cation mixing

between the Li layer and Ni layers during cycling can destabilize the structure. It was reported[39] that the $Li_{1-x}Ni_{0.8}Co_{0.15}Al_{0.05}O_2$ type cathode retains a more stable structure, compared to $LiNiO_2$ until about 0.6 lithium ions are extracted, then the 2-D character of this structure rapidly decreases when x>0.6. The charge passed to the 4.2V cut-off voltage used in this work is close to that for the relatively unstable structural region.

Based on the discharge capacity of 1.22 mAh/cm^2 (160mAh/g) and on the calibration of voltage (OCV) *vs.* state of charge (SOC) for the $Li_{1-x}Ni_{0.8}Co_{0.15}Al_{0.05}O_2$ material, in fact 0.6 Li ions are extracted from the cathode charged to 4.2V.Although extraction of about 0.6 Li from this cathode may not cause severe degradation to the bulk structure, it could produce formation of an unstable and highly reactive lattice. Manthiram and co-workers[41,42] have reported that $Li_{1-x}Ni_{0.85}Co_{0.15}O_2$ loses lattice oxygen when chemically delithiated to x > 0.6-0.7. As they stated in Ref. 41, in the case of electrochemical delithiation in an electrochemical cell, molecular oxygen would not be evolved, rather reaction of the cathode material with the electrolyte may be expected. The effect of Al doping on the stability of lattice oxygen is not known. But unstable lattice oxygen formed at 4.2 V in this cathode material might be expected to react with the electrolyte.

Spectra of the cathode charged to 3.75V before DMC washing are shown in Fig. 6(c). Unwashed cathode exhibits only strong vibration bands of the EC:$LiPF_6$ solvate from the electrolyte, as observed in control experiments with a Au foil and virgin cathode soaked in electrolyte. We suggest that the report by Genies et al.[6] of polycarbonate formation on the surface of mesocarbon microbead (MCMB) anodes charged in EC/$LiPF_6$ electrolyte and examined ex-situ by FTIR is fundamentally a

misinterpretation. Their spectrum for the so-called SEI layer (Fig. 13 in ref. 6) is essentially identical to our spectra in Figure 3 for the solvate on the Au foil.

There was no indication of any species other than the EC:$LiPF_6$ solvate on the surface of the cathode charged to 3.75 V, i.e. the process(s) producing the peak near 3.6 V in the charging curve (Fig. 5) on the first charge did not produce a product observable by IR. The same was true of cathodes charged to potentials between 3.75 and 4.1 V. However, new spectral features were observed on the surface of the unwashed cathode charged to 4.2 V. Those new features are marked in arrows in curve (d) in Fig.6. In addition to the new features in the C=O stretching region between 1800-1700 cm^{-1}, two new peaks appear at ~ 1200 cm^{-1} and 1084 cm^{-1}. The bands at 1805 cm^{-1} and 1775 cm^{-1} could come from a dicarboxylic anhydride[34,35], as shown by the reference spectrum in Figure 7 for maleic anhydride. The simultaneous appearance of three bands of nearly equal intensity at ca. 1750, 1200 and 1080 cm^{-1} indicates, in general, the presence of esters[34,35] of carboxylic acids, RCOOR', where the first band comes from carbonyl C=O stretch, the second from asymmetric C-O-C stretching, and the third involves the ester oxygen and carbon in an asymmetric stretch (O-C-C) mode. The reference spectrum of propionic acid ethyl ester in Figure 7 shows these characteristic features as an example. The reference compound spectra shown in Figure 7 were obtained with our spectrometer in the same ATR geometry as the spectra from the cathode materials. Similar functionalities (a dicarboxylic acid anhydride and/or a (poly)ester) were observed by K. Kanamura et al.[16] from *in-situ* FTIR experiments as electrochemical oxidation products of propylene carbonate containing $LiPF_6$ or $LiBF_4$ on $LiCoO_2$ cathodes in the "overcharge" potential region 4.2 – 4.8 V.

The spectra of the cathodes following DMC washing are shown in Figure 8 along with that of the control cathode (soaked in electrolyte but not charged or discharged) and a polyether reference sample. Gentle rinsing (10 seconds) with DMC resulted in much reduced intensity of the peaks in the 1700 – 1850 cm^{-1} region, and all features were eliminated by another (10 second) rinse. Only the peaks of PVdF, already present in the virgin cathode laminate, were observed from the cathodes washed in DMC. PEO has a unique strong absorption band for the C-O-C (ether) asymmetric stretching at 1104 cm^{-1}, well-resolved from the vibrational bands of PVdF, which makes it relatively easy to detect by FTIR. Such features were clearly *not* observed in the rinsed cathodes. Still we could not rule out the possibility of a C-O-C (ether) functionality on the un-washed cathode, since the absorption from the EC:$LiPF_6$ residue on unwashed cathodes was so strong that features from other species on the cathode surface could be severely attenuated. Nevertheless, polymers such as PEO or polyethercarbonate, if indeed formed on the cathode after electrochemistry, should still be observable after DMC washing, and they are not. The reaction products (a dicarboxylic acid anhydride and/or alkyl ester) that do form on the surface of the cathode at 4.2 V are easily rinsed from the surface by DMC. Note that the signatures of Li_2CO_3 are absent in the cathode spectra in Fig. 7, confirming the decomposition of the Li_2CO_3 at some point in time in these experiments. The major product of $LiPF_6$ decomposition has been reported to be LiF, as observed by NMR, X-ray photoelectron and X-ray absorption spectroscopic analyses[21-23]. Unfortunately, LiF is invisible in the mid-IR (700-4000 cm^{-1}) region, and could not be observed in our experiments.

In other experiments from this laboratory using in-situ FTIR, we found that CO_2 gas evolved from a glassy carbon working electrode in this identical EC/DEC electrolyte only at potentials above 5.2 V, well above the 4.2 V cut-off used here and in Li-ion batteries in general. No surface products could be detected on a glassy carbon electrode at potentials below 5.2 V, consistent with the in-situ FTIR study by Kanamura et al. for PC/$LiClO_4$ with "inert" Pt and Au electrodes. DFT quantum chemical calculations have shown[27] that ionization of cyclic carbonates like EC and PC forms an unstable radical cation, and that the most energetically favorable reaction path is dissociation into CO_2 and the radical cation of ethylene oxide ($\bullet C_2H_4O^+$). In the condensed phase, the latter could react with EC to form a poly(ether)carbonate, in the manner of Lewis acid catalyzed polymerization of EC (which also generates CO_2 as a co-product)[43,44]. However, poly(ether)carbonate was not observed as a product in these experiments. At lower potentials at oxide cathodes, there appears to be another solvent oxidation path that is not initiated by *ionization* of the solvent molecule, but by a chemical interaction of the solvent molecule with the oxide surface. The reaction appears to be an *indirect* electrochemical oxidation, where removal of Li ions in this material at 4.2 V destabilizes oxygen anions in the oxide lattice[41,42], resulting in a highly reactive state and oxygen transfer from the oxide to the solvent.

Conclusions

FTIR analysis of Gen2 cathodes, charged from 3.75 to 4.2V vs. Li/Li^+ in the electrolyte of EC:DEC(1:1) - 1M $LiPF_6$, indicated formation of an organic surface layer containing dicarbonyl anhydride and carbonyl ester (RCOOR') functional groups, but only at 4.2 V. The surface layer was removed by rinsing with DMC. As a result, only PVdF and a

polyamide from the Al current collector remained after washing and drying at room temperature. A pre-existing surface layer of Li_2CO_3 present in the virgin cathode was eliminated just by storing in the electrolyte, and no Li_2CO_3 was found on the cathode after cycling. The reaction at 4.2 V appears to be an indirect electrochemical oxidation where overcharging ($x > 0.6$) destabilizes oxygen in the oxide lattice resulting in oxygen transfer from the oxide surface to the solvent molecules.

Acknowledgments

This work was supported by the Office of Advanced Automotive Technologies of the U. S. Department of Energy under contract No. DE-AC03-76SF00098. We would like to thank K. A. Striebel for supplying the Gen2 cathode material, J. Shim for his assistance in electrochemical experiments, and John Kerr for critical discussions.

References

1. E. Peled, in *Lithium Batteries*, Chapt. 3, J. P. Gabano, Editor, Academic Press, London (1983).
2. M. Winter, J. O. Besenhard, M. E. Spahr and P. Novak, *Adv. Mater.* , **10**, 725 (1998).
3. A. N. Dey, B. P. Sullivan, *J. Electrochem. Soc.*, **117**, 222 (1970).
4. R. Fong, U. von Sacken, J. R. Dahn, *J. Electrochem. Soc.*, **137**, 2009 (1990).
5. A. C. Chu, J. Y. Josefowicsz, G. C. Farrington, *J. Electrochem. Soc.*, **144**, 41612 (1997)
6. S. Geniès, R. Yazami, J. Garden and J. C. Frison, *Synth. Metals*, **93**, 77 (1998)
7. D. D. MacNeil, D. Larcher, J. R. Dahn, *J. Electrochem. Soc.*, **146**, 3596 (1999).
8. D. Aurbach, *J. Power Sources*, **89**, 206 (2000).
9. O. Chusid, Y. Gefer, D. Aurbach, M. Watanabe, T. Momma, T. Osaka, *J. Power Sources*, **97-98**, 632 (2001)

10. K. I. Morigaki, *J. Power Sources*, **103**, 253 (2002).

11. X. Zhang, P. N. Ross, Jr., R. Kostecki, F. Kong, S. Sloop, J. B. Kerr, K. Striebel, E. J. Cairns, F. McLarnon, *J .Electrochem. Soc*., **148**, A463 (2001).

12. D. D. MacNeil and J. R. Dahn, *J. Electrochem. Soc.*, **148**, A1205 (2001).

13. D. D. MacNeil and J. R. Dahn, *J. Electrochem. Soc.*, **148**, A1211 (2001).

14. K. Kanamura, *J. Power Sources*, **81-82**, 123 (1999).

15. K. Kanamura, S. Tohyama, S. Shiraishi, M. Ohashi, Z. Takehara, *J. Electroanal. Chem.*, **419**, 77 (1996).

16. K. Kanamura, T. Umegaki, M. Ohashi, S. Toriyama, S. Shiraishi and Z. Takehara, *Electrochim. Acta*, **433**, 47 (2001).

17. D. Aurbach, K. Gamolsky, B. Markovsky, G. Salitra, Y. Gofer, U. Heider, R. Oestern, M. Schmidt, *J. Electrochem. Soc*., **147**, 1322 (2000).

18. Z. Wang, X.Huang, L. Chen, *J. Electrochem. Soc*., **150**, A199 (2003).

19. D. Aurbach, *J. Power Sources*, **81-82**, 95 (1999).

20. D. Aurbach, *J. Power Sources*, **89**, 206 (2000).

21. M. Balasubramanian, H. S. Lee, X. Sun, X. Q. Yang, A. R. Moodenbaugh, J. McBreen, D. A. Fischer, Z. Fu, *Electrochem. Solid-State Lett*., **5**, A22 (2002).

22. Y. Wang, X. Guo, S. Greenbaum, J. Liu, K. Amine*, Electrochem. Solid-State Lett*., **4**, A68 (2002).

23. A. M. Andersson, D. P. Abraham, R. Haasch, S. MacLaren, J. Liu and K. Amine, *J. Electrochem. Soc.*, **149**, A1358 (2002).

24. T. Eriksson, A. M. Andersson, A. G. Bishop, C. Gejke, T. Gustafsson and J. O. Thomas, *J. Electrochem. Soc.*, **149**, A69 (2002).

25. L. Vogdanis and W. Heitz, *Macromol. Rapid Commun.*, **7**,543 (1986); L. Vogdanis, B. Martens, H. Uchtmann, F. Hensel and W. Heitz, *Macromol. Chem.*, **191**, 465 (1990).

26. D.P.Abraham, R.D. Twesten, M. Balasubramanian, J. Kropf, D. Fischer, J. McBreen, I. Petrov, and K. Amine, *J. Electrochem. Soc.*, **150**, A1450(2003)

27. X. Zhang, J. K. Pugh and P. N. Ross, *J. Electrochem. Soc.*, **148**, E183 (2001).

28. M. Moshkovic, M. Cojocaru, H.E. Gottlieb, and D. Aurbach, *J. Electroanal. Chem.* **2001**, *497*, 84.

29. F. Joho and P. Novak, *Electrochim. Acta* **2000**, *45*, 3589.

30. G. V. Zhuang and P. N. Ross, Jr., *Electrochem. Solid-State Lett.*, **6**, 1 (2003).

31. PNGV Battery Test Manual, DOE/ID-10597, Revision 3, February, 2001.

32. I. Bloom, B.W. Cole, J.J. Sohn, S.A. Jones, E.G. Polzin, V.S. Battaglia, G.L. Hendrikson, C. Motlock, and R. Richardson, *J. Power Sources*, **101**, 238 (2001).

33. K. Matsumoto, R. Kuzuo, K. Takeya and A. Yamanaka, *J. Power Sources*, **81-82**, 558 (1999).

34. D. Lin-Vien, N. B. Colthup, W.G. Fately, J.G. Graselli, *The Handbook of Infrared and Raman Characteristic Frequencies of Oragnic Molecules*, Academic Press, San Diego, 1991.

35. N. B. Colthup, L.H. Daly and S.E. Wiberley, *Introduction to Infrared and Raman Spectroscopy*, 3rd edition, Academic Press, San Diego, 1990.

36. Aldrich Handbook of Fine Chemicals and Laboratory Equipment, 2003, p.1494.

37. B. Fortunato, P. Mirone, G. Fini, *Spectrochim. Acta*, **27A**, 1917 (1971).

38. J. Shim, R. Kostecki, T. Richardson, X. Song and K. A. Striebel, *J. Power Sources*, **112**, 222 (2002).

39. K. K. Lee, W. S. Yoon, K. B. Kim, K. Y. Lee and S. T. Hong, *J. Power Sources*, **97-98**, 308 (2001).

40. R.V. Chebiam, F. Prado, and A, Manthiram, *J. Electrochem. Soc.*, **148**, A49 (2001).

41. R.V. chebiam, A.M. Kannan, F. Prado and A. Manthiram, *Electrochem. Commun*., **3**, 624 (2001).

42. S. Venkatraman, Y. Shin and A. Manthiram, *Electrochem. Solid State Lett.*, **6**, A9 (2003).

43. S. E. Sloop, J. K. Pugh, S. Wang, J. B. Kerr and K. Kinoshita, *Electrochem. Solid State Lett.*, **4**, A42 (2001).

44. L. Vogdanis, B. Martens, H. Uchtmann, F. Hensel, and W. Heitz, *Makromol. Chem.*, **191**, 465 (1990); L. Vogdanis and W. Heitz, *Makromol. Chem. Rapid Commun.*, **7**, 543 (1986).

Figure captions

Figure 1. IR spectra of the as-received Gen2 cathode $LiNi_{0.8}Co_{0.15}Al_{0.05}O_2$ and PVdF used as a binder for the cathode laminate; spectrum of Li_2CO_3 also shown for reference.

Figure 2. (lower) Comparative IR spectra of as-received Gen2 cathode, an Al foil used as a current collector for the cathode laminate and a reference spectrum of oleamide, a common corrosion inhibitor. (upper) Comparison of C-H stretching region of the spectra of the virgin cathode and the film on the Al foil current collector used in the cathode.

Figure 3. IR spectra of electrolyte residue on a Au foil soaked in electrolyte without electrochemistry: (a) before washing with DMC (b) at a different spot and (c) after washing with DMC and drying at room temperature.

Figure 4. IR spectra of: (a) as-received Gen2 cathode; (b) soaked in the electrolyte without electrochemistry before washing and (c) after washing with DMC and drying in glove box at room temperature; (d) the PVdF binder by itself.

Figure 5. (top) Voltage profile of a Gen2 cathode $LiNi_{0.8}Co_{0.15}Al_{0.05}O_2$ charged/discharged at about the C/25 rate and (bottom) the differential capacity curve.

Figure 6. Selected IR spectra of samples before DMC washing: (a) electrolyte residue on Au foil; (b) electrolyte residue on as-received Gen2 cathode without electrochemistry; (c) Gen2 cathode charged to 3.75 V; (d) Gen2 cathode charged to 4.20 V. New features appearing in the spectrum (d) are marked by arrows.

Figure 7. IR spectra of: (a) propionic acid methyl ester; (b) maleic anhydride; (c) Gen2 cathode charged to 3.75 V not washed; (d) Gen2 cathode charged to 4.2 V not washed.

Figure 8. IR spectra of GEN2 cathodes after rinsing with DMC compared with that for just the PVdF binder.

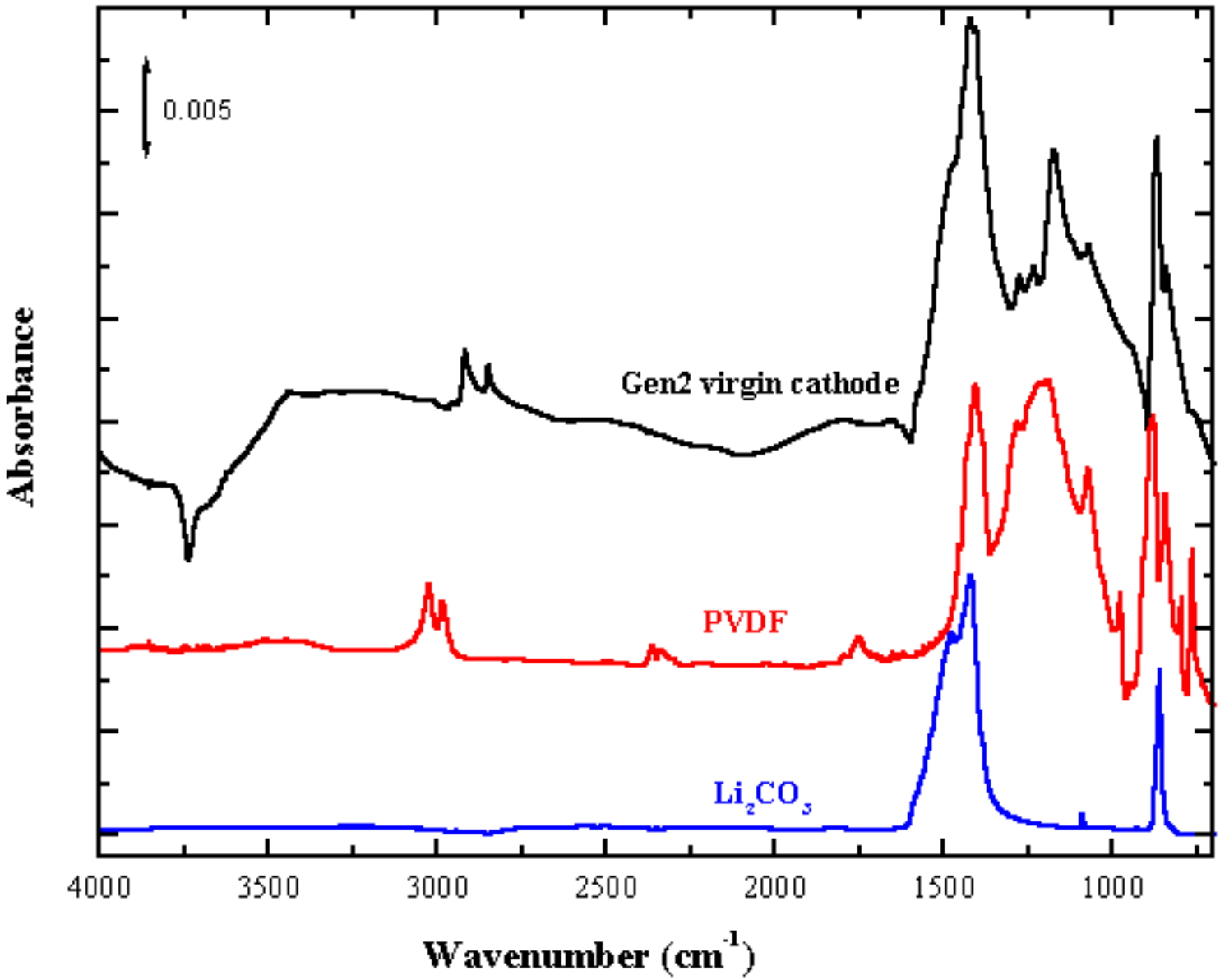
0.005
Gen2 virgin cathode
PVDF
Li_2CO_3
Absorbance
4000
3500
3000
2500
2000
1500
1000
Wavenumber (cm^{-1})

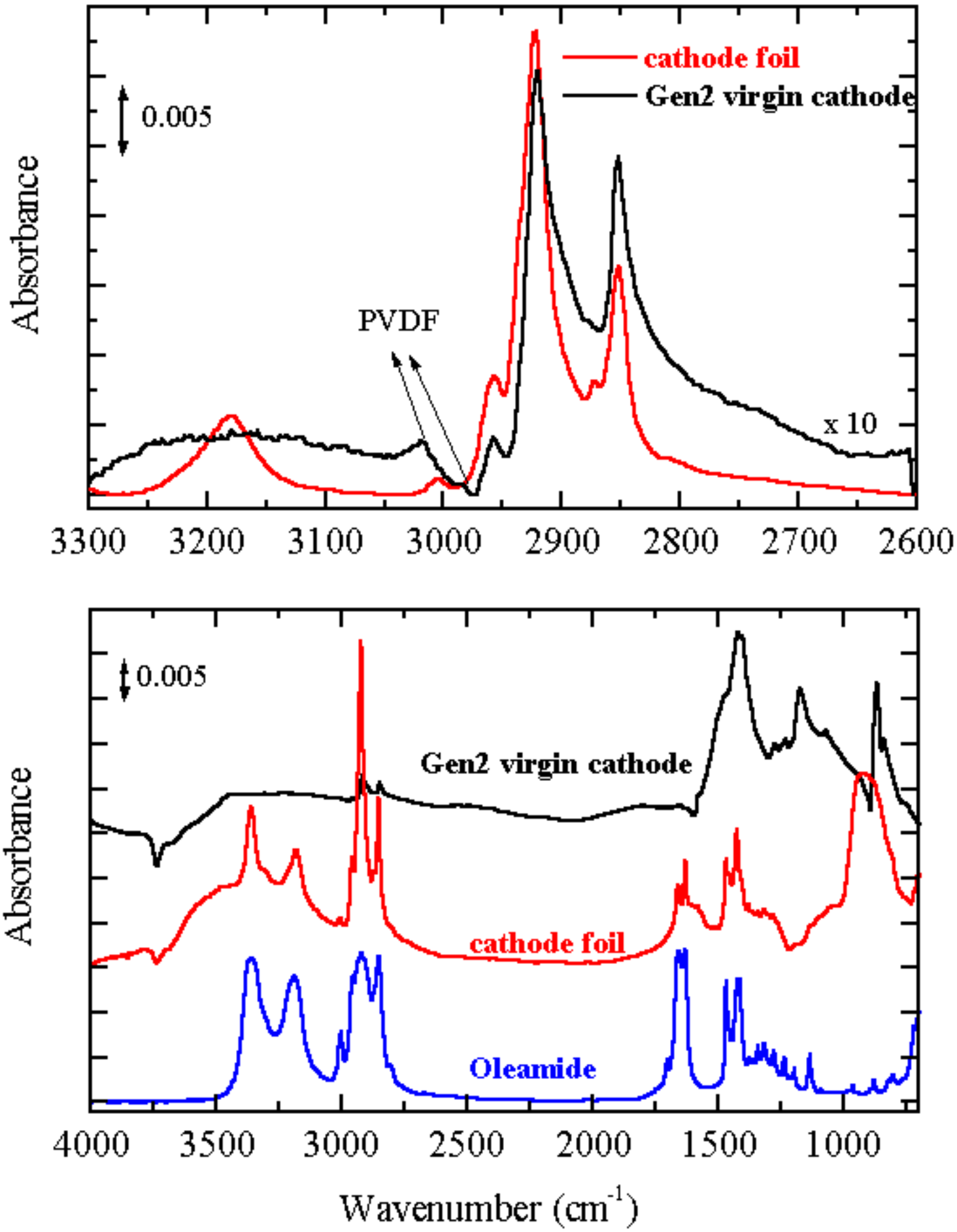
cathode foil
Gen2 virgin cathode
0.005
Absorbance
PVDF
x 10
3300
3200
3100
3000
2900
2800
2700
2600
0.005
Gen2 virgin cathode
Absorbance
cathode foil
Oleamide
4000
3500
3000
2500
2000
1500
1000
Wavenumber (cm-1)

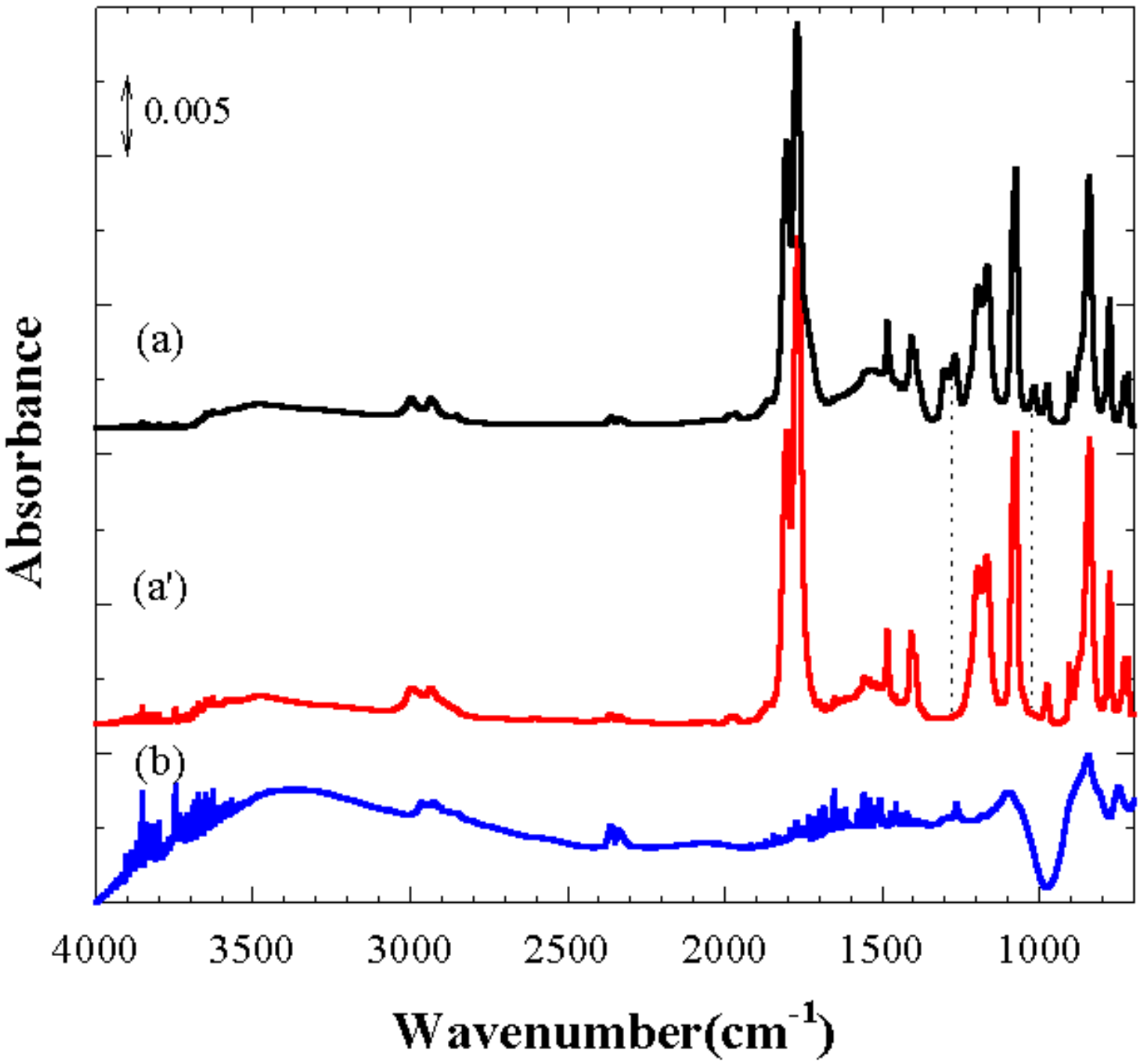
0.005
(a)
(a′)
(b)
Absorbance
4000
3500
3000
2500
2000
1500
1000
Wavenumber(cm-1)

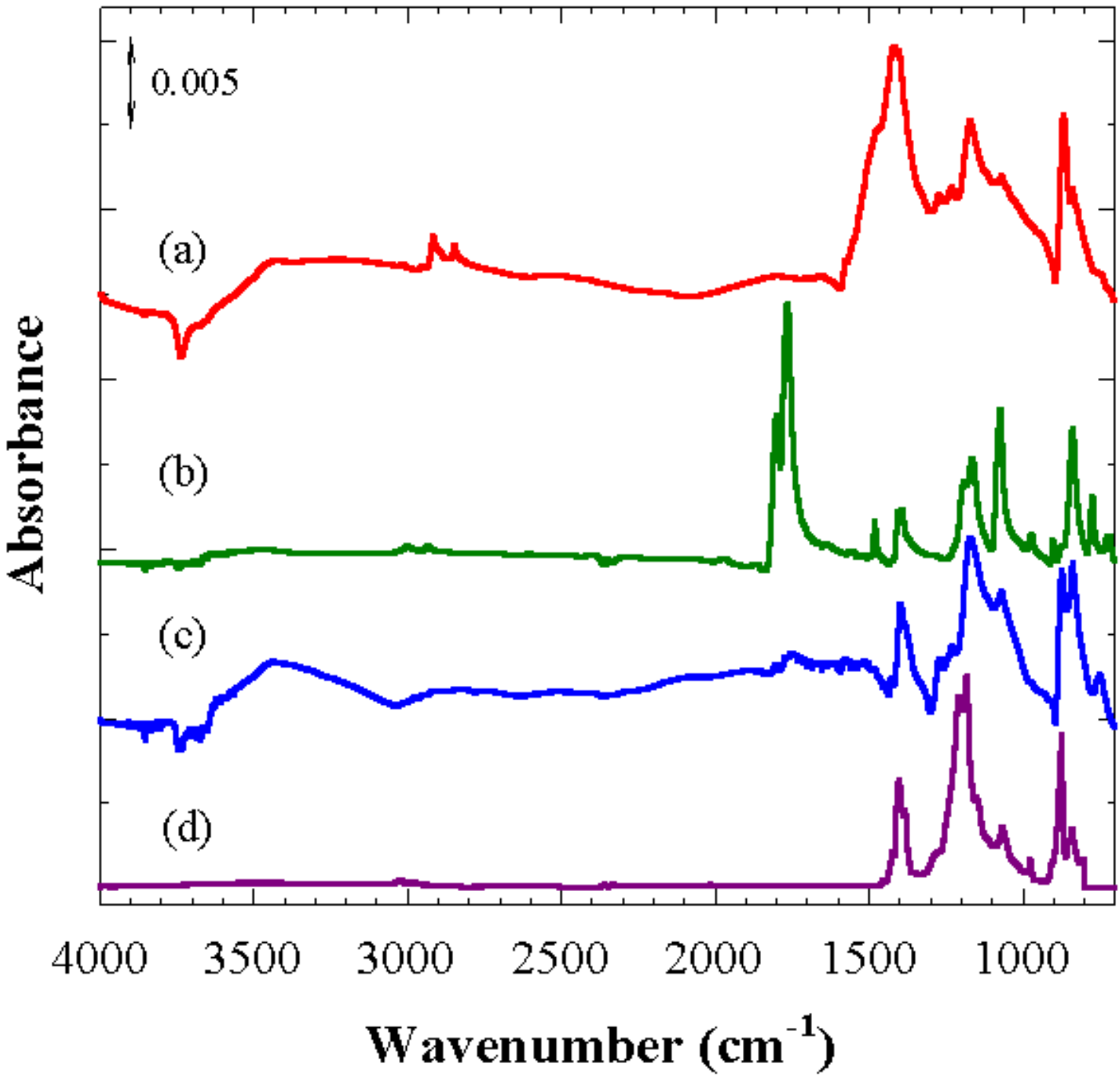
0.005
(a)
(b)
(c)
(d)
Absorbance
4000
3500
3000
2500
2000
1500
1000
Wavenumber (cm-1)

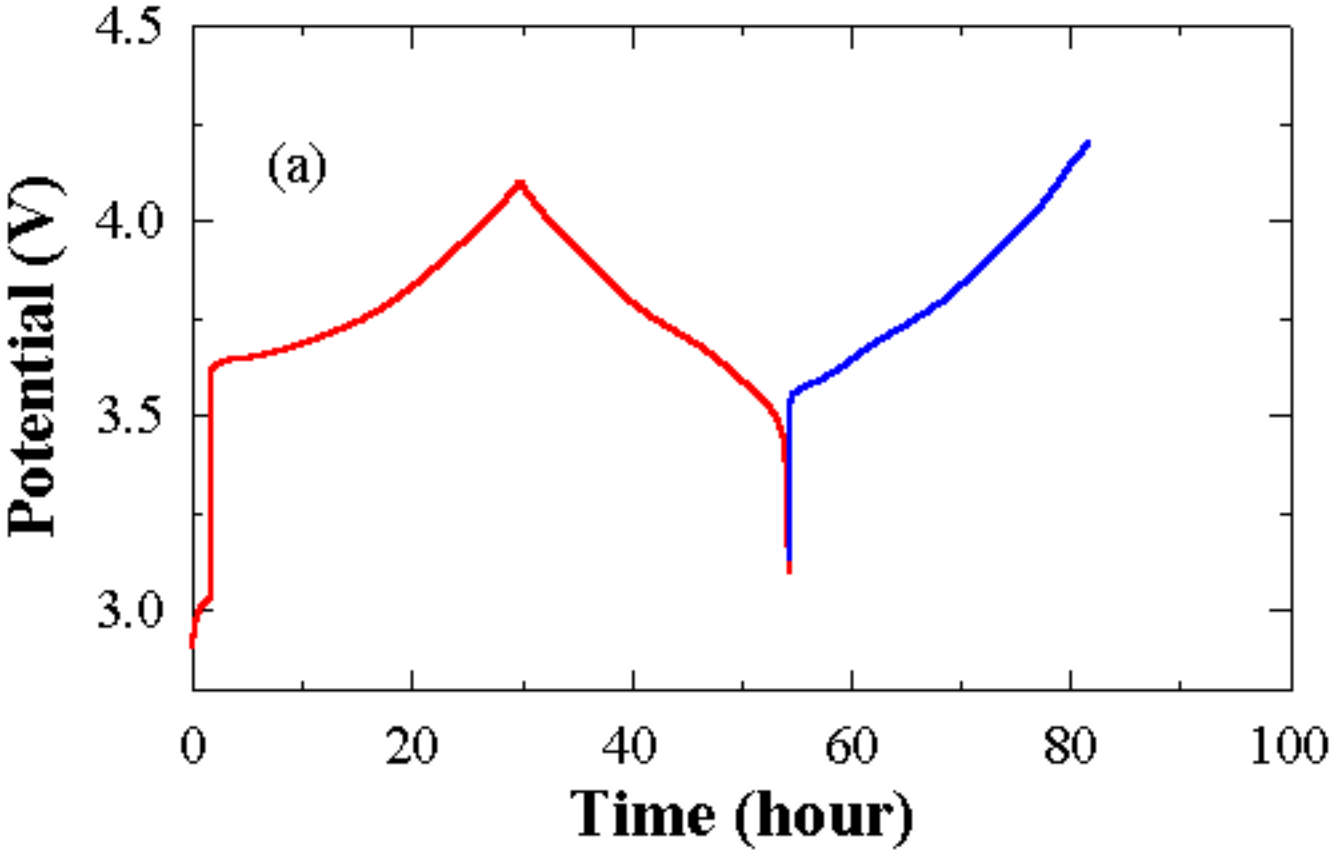
(a)
Potential (V)
4.5
4.0
3.5
3.0
0
20
40
60
80
100
Time (hour)

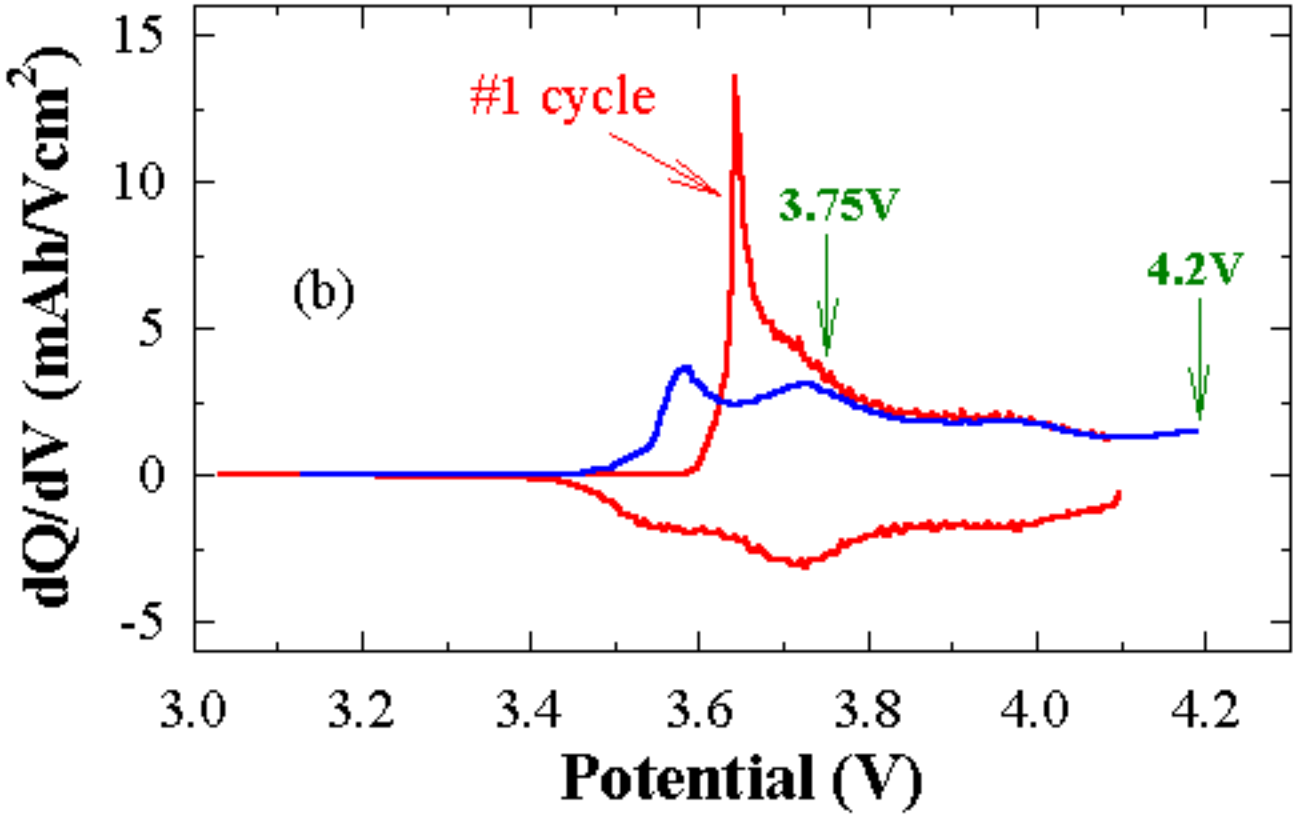
(b)
#1 cycle
3.75V
4.2V
dQ/dV (mAh/Vcm^2)
15
10
5
0
-5
3.0
3.2
3.4
3.6
3.8
4.0
4.2
Potential (V)

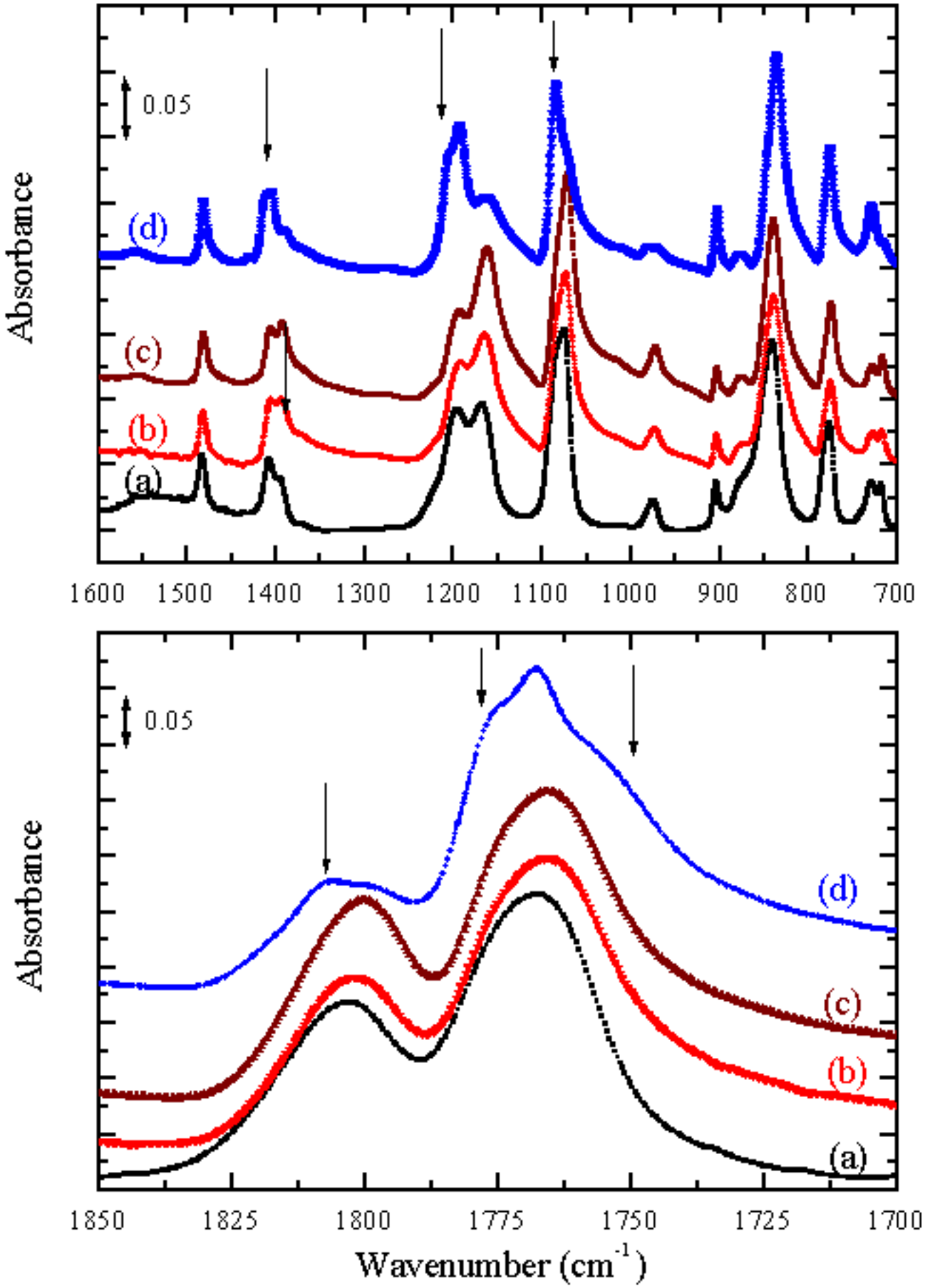
0.05
Absorbance
(d)
(c)
(b)
(a)
1600
1500
1400
1300
1200
1100
1000
900
800
700
0.05
Absorbance
(d)
(c)
(b)
(a)
1850
1825
1800
1775
1750
1725
1700
Wavenumber (cm-1)

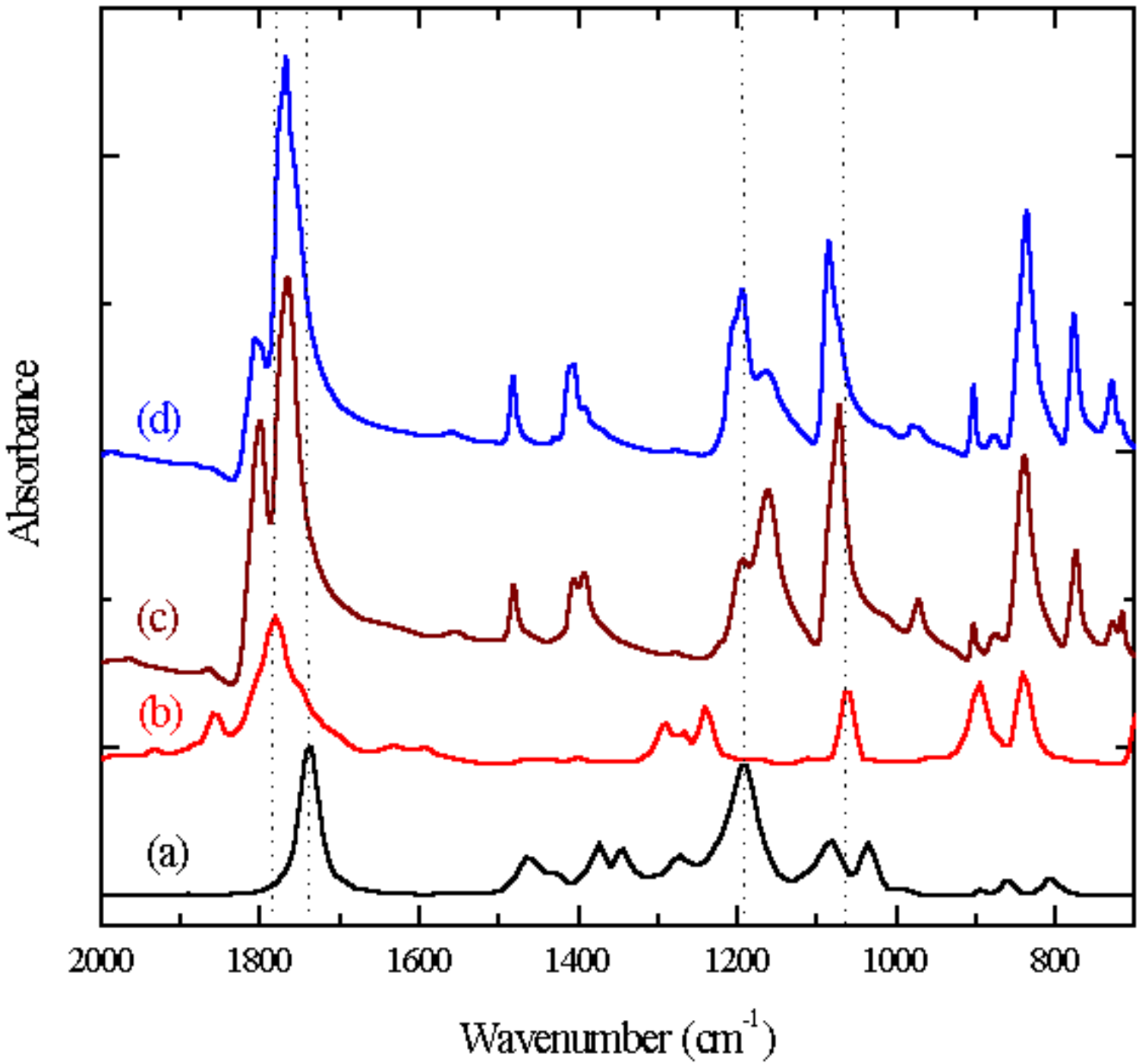
Absorbance
(d)
(c)
(b)
(a)
2000
1800
1600
1400
1200
1000
800
Wavenumber (cm-1)

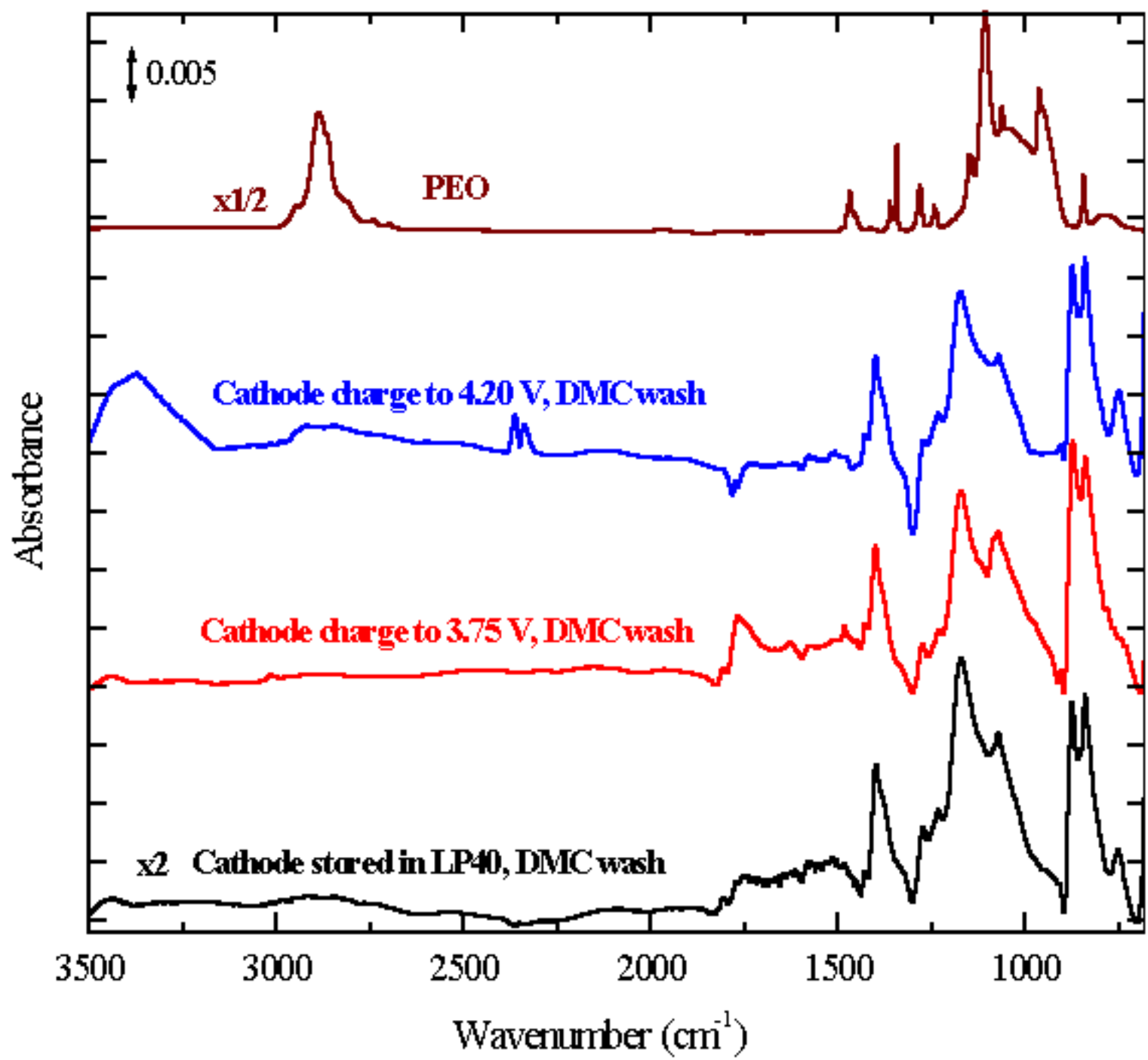
0.005
x1/2
PEO
Cathode charge to 4.20 V, DMC wash
Cathode charge to 3.75 V, DMC wash
x2
Cathode stored in LP40, DMC wash
Absorbance
3500
3000
2500
2000
1500
1000
Wavenumber (cm-1)